Expeditious Preparation of Open-Cage Fullerenes by Rhodium(I)-Catalyzed [2+2+2] Cycloaddition of Diynes and C_{60}: an Experimental and Theoretical Study

Albert Artigas, Anna Pla-Quintana, Agustí Lledó,* Anna Roglans,* and Miquel Solà*[a]

Abstract: A novel methodology to transform C_{60} into a variety of open-cage fullerene derivatives employing rhodium(I) catalysis has been developed. This transformation encompasses a partially intermolecular [2+2+2] cycloaddition reaction between diynes **1** and C_{60} to deliver a cyclohexadiene-fused fullerene, which concomitantly undergoes a formal [4+4]/retro-[2+2+2] rearrangement to deliver open-cage fullerenes **2**. Most notably, this process occurs without the need of photoexcitation. The complete mechanism of this transformation has been rationalized by DFT calculations, which indicate that, after [2+2+2] cycloaddition, the cyclohexadiene-fused intermediate evolves into the final product through a Rh-catalyzed di-π-methane rearrangement followed by a retro-[2+2+2] cycloaddition. The obtained open-cage fullerenes can be derivatized by Suzuki-Miyaura cross-coupling, or subjected to ring expansion to deliver a 12-membered ring orifice in the fullerene structure. Overall, the methodology presented constitutes a straightforward entry to functional open-cage C_{60}-fullerene derivatives employing catalytic methods.

Introduction

Functionalized C_{60} fullerenes, in which the properties of C_{60} can be combined with those of other classes of materials, are an important type of scaffolds with relevant applications in several fields, such as material science, nanotechnology and medicinal chemistry among others.[1] In particular, carbocyclic fullerene adducts with fused-ring systems have been studied in the field of organic photovoltaic solar cells.[2] Open-cage fullerenes, which result from selective cleavage of one or more fullerene carbon-carbon bonds, are particularly interesting structures since they can act as host molecules encapsulating guests within their cavity, thereby forming endohedral complexes with emerging properties and particular reactivity.[3] From the practical point of view, open-cage derivatives of C_{60} have proven useful as electron accepting materials in organic solar cells[4] and as ligands for the synthesis of metal complexes.[5] The photoinduced ring-opening reaction of cyclohexadiene-fused C_{60} derivatives by tandem [4+4]/retro-[2+2+2] rearrangement is one of the most well-established synthetic entries to open-cage fullerenes.[6] For all these reasons, the development of efficient synthetic routes to fullerene derivatives is still an appealing goal in organic synthesis. On the other hand, transition-metal catalyzed [2+2+2] cycloaddition reactions appear as the method of choice for the synthesis of six-membered rings and enable the construction of cyclohexadiene scaffolds when the reaction takes place between two alkynes and one alkene.[7] Given that the chemical reactivity of C_{60} is typical of an electron-deficient olefin it appears as a valuable candidate as a co-substrate in [2+2+2] cycloaddition with alkynes.[7a] Furthermore, cycloaddition reactions in empty fullerenes show a remarkable preference to [6,6] ring junction over [5,6] bonds.[1c,8]

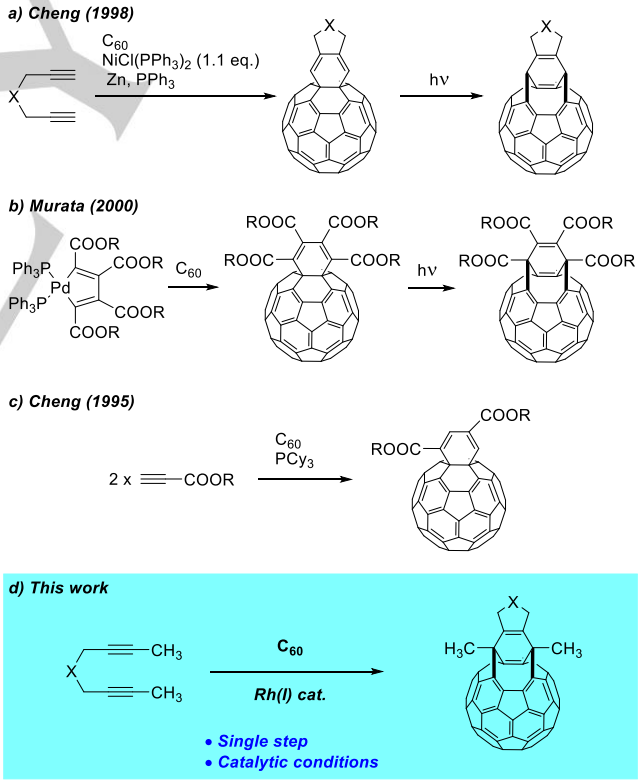

Scheme 1. Approaches to cyclohexadiene-fused and open-cage fullerenes derivatives.

To the best of our knowledge, only two previous studies have reported transition-metal promoted [2+2+2] cycloaddition reactions of two alkynes with C_{60} while using stoichiometric amounts of the transition metal species (Scheme 1). The first,

[a] A. Artigas, Dr. A. Lledó, Dr. A. Pla-Quintana, Prof. Dr. A. Roglans, Prof. Dr. M. Solà
Institut de Química Computacional i Catàlisi (IQCC) and Departament de Química, Universitat de Girona
C/ Maria Aurèlia Capmany, 69, 17003, Girona, Catalonia (Spain)
E-mail: agusti.lledo@udg.edu, miquel.sola@udg.edu, anna.roglans@udg.edu

Supporting information for this article is given via a link at the end of the document.

published in 1998 by Cheng et al.,[9] described the cycloaddition of terminal diynes with C_{60} using excess amounts of a nickel precursor in order to avoid the gradual decomposition of the complex. In this study, the corresponding cyclohexadiene-fused derivatives were isolated and characterized. After irradiation with a 350 nm UV lamp, these compounds rearranged into the corresponding bis(fulleroids) (i.e. compounds in which two C–C bonds of the original C_{60} cage have been broken). The authors found that these fulleroids were thermally and photochemically more stable than their cyclohexadiene counterparts. The second, by Murata et al. in 2000,[10] described the reaction of fullerene with a palladacyclopentadiene –previously prepared by oxidative coupling of two molecules of a dialkyl acetylenedicarboxylate with Pd(0)–, affording the corresponding cyclohexadiene-type adducts. In an early study by Cheng et al.,[11] a metal-free cyclotrimerization of ethyl propiolate with fullerene promoted by PCy_3 was described (Scheme 1). However, this transformation operates on a different reaction manifold that is limited to Michael acceptors. Based on our previous experience in Rh-catalyzed [2+2+2] cycloaddition reactions between alkynes and both alkenes and allenes,[12,7b] we envisaged to develop a catalytic version of the [2+2+2] cycloaddition reaction between diynes and fullerene. Subsequent [4+4] photocycloaddition and retro-[2+2+2] reaction of the cyclohexadiene derivatives would provide, overall, a versatile and efficient entry to open-cage fullerenes. Based on our previous theoretical DFT study that showed the viability of a rhodium-catalyzed [2+2+2] cycloaddition reaction of two alkynes and C_{60},[13] we present here a successful implementation of this methodology that affords open-cage fullerenes in a single reaction step.

Results and Discussion

At the onset, a variety of reaction conditions for the model cycloaddition between fullerene C_{60} and non-terminal *N*-tosyl tethered diyne **1a** were explored (Table 1). Eventually, we found that a 10% mol of a mixture of a cationic rhodium complex with Tol-BINAP (**P1**) as a diphosphine in *o*-dichlorobenzene at 90 °C for 4 hours afforded a 52% isolated yield of a dark brown solid. The mixture of $[Rh(cod)_2]BF_4$ and Tol-BINAP was treated with hydrogen in dichloromethane (DCM) solution for catalyst activation prior to substrate addition. The molecular formula of the new compound was determined by HRMS to be $C_{75}H_{17}NO_2S$, indicating that the cycloaddition had taken place. 1D and 2D NMR spectroscopic experiments were used to ascertain the structure of the product formed. Both the ^1H and ^{13}C NMR spectra show that the new compound has C_s rather than C_{2v} symmetry, the latter resulting from a cycloaddition reaction at the [6,6] bond. A careful analysis of the NMR data revealed an unanticipated but yet desirable outcome: the compound formed was not the expected cycloadduct, but rather the corresponding open-cage bis(fulleroid) structure (Figure 1). The ^1H NMR exhibits a singlet at δ 2.79 ppm, corresponding to the two methyl groups originating from the starting diyne, and, importantly, two multiplets centered at 4.46 ppm and 4.59 ppm. The latter correspond to two pairs of diastereotopic protons, H3 and H3' respectively, a key feature to identification of the symmetry point group. The ^{13}C NMR showed 35 signals in the sp^2 carbon region (30 from the fullerene core, partially overlapped, 4 from the tosyl group and 1 from the fused double bond) and 4 signals in the sp^3 carbon region at δ 21.8, 27.7, 43.4 and 55.0 ppm. An HMBC experiment was conducted to confirm the open-cage structure. The 2D spectrum displays a two bond correlation between the protons of the methyl group and the Csp^3 at 43.4 ppm and a three bond correlation between the same protons and three Csp^2 quaternary carbon atoms (134.9, 137.4 and 150.2 ppm), proving the accuracy of our earlier observation. The assignment of the most characteristic signals in the ^1H and ^{13}C NMR spectra is shown in Figure 1.

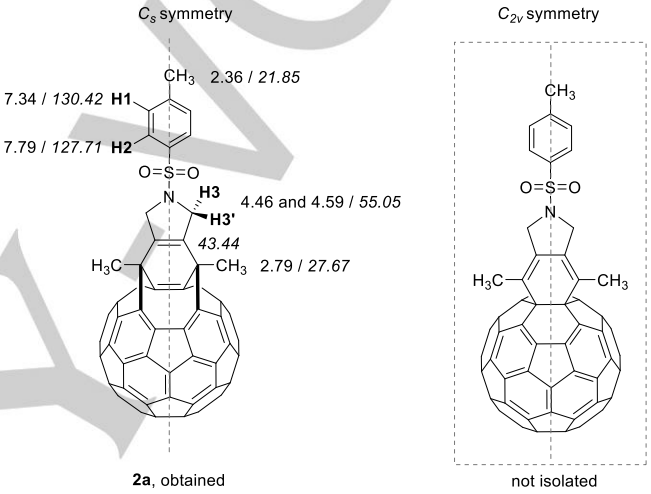

Figure 1. Selected ^1H and ^{13}C (in italics) NMR chemical shifts of **2a**.

Having established a straightforward entry to open-cage fullerenes based on a cascade process triggered by the Rh-catalyzed [2+2+2] cycloaddition and followed by fullerene-cage opening, we next examined the effect that altering various reaction parameters had on the efficiency of the process (Table 1). The Wilkinson catalyst – $[RhCl(PPh_3)_3]$, a neutral rhodium complex – did not promote the reaction even when stoichiometric amounts of catalyst were used (entries 1 and 2, Table 1). We then moved to a combination of a cationic rhodium complex $[Rh(cod)_2]BF_4$ with several phosphines as ligands. BINAP (**P2**) was initially used as benchmark ligand. When the reaction mixture was heated at 90 °C for 4 hours, a 20% yield of cycloadduct **2a** was obtained (entry 3, Table 1). Extending the reaction time to 16 hours did not result in any significant improvement (entry 4, Table 1). Two control experiments were then run, one in the absence of BINAP (entry 5, Table 1) and the other in the absence of Rh complex (entry 6, Table 1), which revealed the essential role of the two components in this transformation. Increasing the reaction temperature to 120 °C (entry 7, Table 1) or using microwave heating at 80 °C for 40 minutes (entry 8, Table 1) did not improve the results. We reasoned that homocoupling reactions of **1a** might effectively compete with the desired cycloaddition pathway, and we ran a reaction slowly adding **1a** to a mixture of fullerene and

the catalytic system at 90 °C. However, again only a 20% yield of **2a** was obtained (entry 9, Table 1). We then turned our attention to other bidentate phosphines: H_8-BINAP (**P3**, entry 10, Table 1), BIPHEP (**P4**, entry 11, Table 1), DTBM-SEGPHOS (**P5**, entry 12, Table 1), DPPE (**P6**, entry 13, table 1), DPPF (**P7**, entry 14, Table 1) and Tol-BINAP (**P1**, entry 16, Table 1). Among these **P1** gave the best results. Finally, MonoPhos (**P8**) – a monodentate phosphoramidite – was also tested, but only traces of **2a** were obtained (entry 15, Table 1). At this point and with the optimal ligand of choice – Tol-BINAP – we proceeded to evaluate the effect of fullerene concentration and diyne excess. We found that both the reduction of fullerene concentration (entry 17, Table 1) and the use of diyne **1a** in excess with respect to fullerene (entry 18, Table 1) improved the yield of the reaction (from 28% to 36% and 43%, respectively). An additive effect was observed when the two factors were combined ([C_{60}] = 1.4 mM and 5 equiv. of **1a**) resulting in our optimized set of conditions (entry 19, Table 1).

Having established the optimum reaction conditions, the scope of the reaction was then evaluated, as shown in Figure 2. In a first step, the nature of the substituents of the phenyl ring at the sulfonamide tether in diyne **1** was evaluated. The corresponding cycloadducts **2b-e** were obtained in excellent yields in all cases, including bromo- and iodobenzene derivatives (**2c-d**) that have the potential for further functionalization (vide infra). A diyne bearing the 5-methyl-2-pyridinesulfonyl group provided **2f** in a 52% isolated yield, indicating that the presence of a potentially coordinating nitrogen atom did not poison or interfere with the catalyst. A sulfonamide tether with aliphatic substitution (trimethylsilylethane) was also efficient, delivering the fulleroadduct **2g** in a 35% isolated yield. Other diynes with diethyl malonate, methylene and oxygen tethers were also tested. However, only the malonate provided good yields of cycloadduct **2h**, while the other two did not furnish any product at all (**2i** and **2j**). Several terminal diynes and others with different substitution at the two termini were then evaluated. The results indicate that alkyne substitution has a dramatic effect on the reaction outcome: only the substrates with at least one internal alkyne gave the corresponding cycloadduct (**2k** and **2o**), albeit in low yields. In the cases of the cycloaddition of diynes **2k**-**2p**, homocoupling of the diyne compete with the cross-coupling with fullerene, especially in the cases that diynes have terminal alkynes such as **2k**, **2l**, **2o**, and **2p**.

Further functionalization of cycloadducts 2. The halogen atom in derivatives **2c** and **2d** opens the door to further functionalizing the fulleroid adducts. Therefore, iodo derivative **2d** was submitted to a Suzuki-Miyaura cross-coupling reaction with *p*-methoxyphenyl boronic acid. After some experimentation, we found that a 10% mol loading of $Pd(PPh_3)_4$ in a mixture of *o*-dihlorobenzene/water 9:1 at 100 ºC in the presence of cesium carbonate as a base provided the best reaction conditions (Scheme 2). Biphenyl derivative **4a** was obtained with a 63% yield.

Table 1. Rhodium(I)-catalyzed cycloaddition of C_{60} with diyne **1a**: effect of reaction parameters.

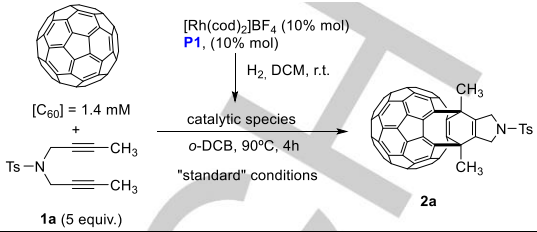

Entry	Deviation from standard conditions	Yield of **2a**[a]
1	$RhCl(PPh_3)_3$, [C_{60}] = 7 mM, 1 eq. **1a**, 16h	0
2	1 eq. $RhCl(PPh_3)_3$, [C_{60}] = 7 mM, 1 eq. **1a**, 16h	0
3	**P2** instead of **P1**, [C_{60}] = 7 mM, 1 eq. **1a**	20
4	**P2** instead of **P1**, [C_{60}] = 7 mM, 1 eq. **1a**, 16h	20
5	No phosphine, [C_{60}] = 7 mM, 1 eq. **1a**, 16h	0
6	No Rh, **P2** instead of **P1**, [C_{60}] = 7 mM, 1 eq. **1a**, 16h	0
7	**P2** instead of **P1**, [C_{60}] = 7 mM, 1eq. **1a**, 120°C	20
8	**P2** instead of **P1**, [C_{60}] = 7 mM, 1 eq. **1a**, 80°C MW heating, 40 min.	10
9	**P2** instead of **P1**, [C_{60}] = 7 mM, slow addition of **1a** (1 eq.) over 4h.	20
10	**P3** instead of **P1**, [C_{60}] = 7 mM, 1 eq. **1a**	20
11	**P4** instead of **P1**, [C_{60}] = 7 mM, 1 eq. **1a**	traces
12	**P5** instead of **P1**, [C_{60}] = 7 mM, 1eq. **1a**	20
13	**P6** instead of **P1**, [C_{60}] = 7 mM, 1eq. **1a**	10
14	**P7** instead of **P1**, [C_{60}] = 7 mM, 1eq. **1a**	traces
15	**P8** instead of **P1**, [C_{60}] = 7 mM, 1eq. **1a**	traces
16	[C_{60}] = 7 mM, 1eq. **1a**	28
17	1eq. **1a**	36
18	[C_{60}] = 7 mM	43
19	**None**	**52**[b]

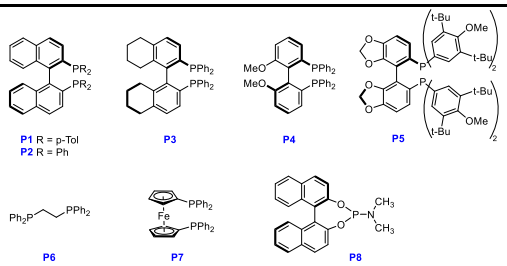

[a] Isolated yield. [b] The yield based on consumed C_{60} was 98%.

Fullerenes and fulleroids can act as mild electron acceptors forming charge-transfer dyads with electron-releasing moieties, such as ferrocene.[14] Moreover, fullerenes appended with photoactive moieties –e.g. pyrene–,[15] can operate as light harvesting antennas through intramolecular energy transfer processes. All these fullerene derivatives constitute promising scaffolds for photovoltaic materials. In this scenario, our Suzuki-Miyaura cross-coupling derivatization appears as an ideal method to append such electron donor or photoactive moieties to fulleroid derivatives. Using the same reaction conditions as for *p*-methoxyphenylboronic acid, 1-pyrenylboronic acid was coupled with cycloadduct **2d** under palladium catalysis to afford derivative **4b** in excellent yield. However, in the case of ferrocene boronic acid, competitive dehalogenation took place, delivering **4c** in a modest 14% yield (Scheme 2).

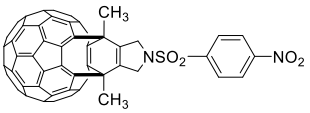

2b (61% isolated yield)
(87% based on consumed C_{60})

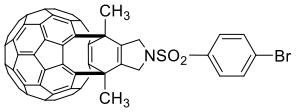

2c (51% isolated yield)
(99% based on consumed C_{60})

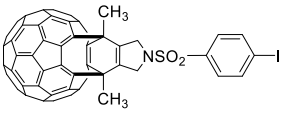

2d (34% isolated yield)
(60% based on consumed C_{60})

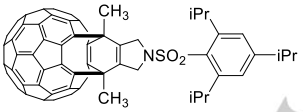

2e (44% isolated yield)
(92% based on consumed C_{60})

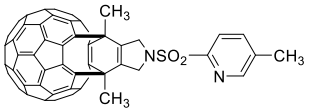

2f (52% isolated yield)
(92% based on consumed C_{60})

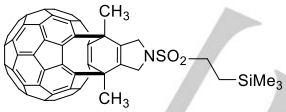

2g (35% isolated yield)
(54% based on consumed C_{60})

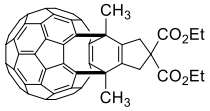

2h (36% isolated yield)
(50% based on consumed C_{60})

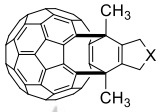

2i (X=CH_2) (0% yield)
2j (X=O) (0% yield)

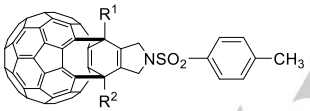

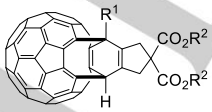

2k (R^1 = CH_3, R^2 = H) (10% isolated yield)
2l (R^1 = H, R^2 = H) (traces)
2m (R^1 = CH_3, R^2 = CO_2CH_3) (traces)
2n (R^1 = Ph, R^2 = Ph) (0%)

2o (R^1 = CH_3, R^2 = CH_3)
(12% isolated yield)
2p (R^1 = H, R^2 = CH_2CH_3) (traces)

Figure 2. Scope of the [2+2+2] cycloaddition of C_{60} with diynes **1**. Reaction conditions: 0.07 mmol of fullerene, 5 equivalents of diyne **1**, 10% mol of Rh catalyst in 50 mL of o-dichlorobenzene (o-DCB) at 90 °C for 4h. The 10% mol mixture of $[Rh(cod)_2]BF_4$ and Tol-BINAP was treated with hydrogen in dichloromethane (DCM) solution for catalyst activation prior to substrate addition.

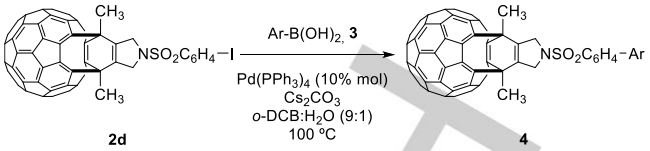

2d 4

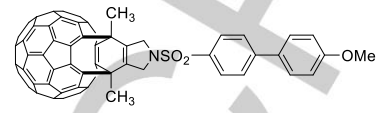

4a (63% yield)

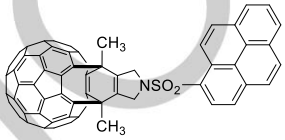

4b (75% yield)

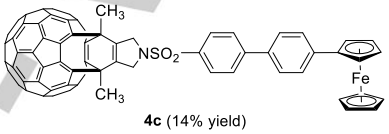

4c (14% yield)

Scheme 2. Suzuki-Miyaura cross-coupling reaction between iodo-fulleroid derivative **2d** with several boronic acids **3a-c.** Reaction conditions: 0.054 mmol of **2d**, 2 equivalents of boronic acid **3**, 2.5 equivalents of Cs_2CO_3, 10% mol of $Pd(PPh_3)_4$ in 10 mL of a mixture of *o*-dichlorobenzene:water (9:1) at 100 °C for 4h.

Oxidative cleavage of fulleroid derivative 2a. As previously described for other open-cage fullerene derivatives,[16] one of the double bonds in the 8-membered ring orifice in **2a** can undergo oxidative cleavage via a photooxygenation process that affords an open-cage fullerene with a 12-membered ring opening containing two carbonyl carbon atoms, **5**. Upon exposure of a $CDCl_3$ solution of **2a** in an NMR tube to sunlight and air for 5 hours, only compound **5** was observed by NMR and HRMS analyses (Scheme 3). The molecular formula of **5** was determined to be $C_{75}H_{17}NO_4S$ by HRMS, indicating the addition of O_2 to **2a**. The color of a solution of compound **5** in chloroform is brown-yellow and the UV-vis spectrum showed maximum absorptions at 254 and 322 nm, whereas the starting compound **2a** is purple in chloroform solution, displaying maxima at 262, 326 and 520 nm. The two UV-vis spectra were similar, but the lack of absorption at 520 nm in **5** indicates the cleavage of one of the aromatic double bonds of the C_{60} and its replacement by two carbonyl groups, disrupting the π-conjugated system of the C_{60} core. NMR analysis revealed the loss of molecular symmetry in the process. The ^{1}H NMR exhibited two different methyl groups at δ 2.21 ppm (C7) and 2.57 ppm (C8), and the ^{13}C NMR displayed two signals corresponding to two different carbonyl groups at 191.5 ppm (C10) and 201.5 ppm (C9). In addition, the two quaternary sp^3 carbons, C6 and C5, appeared at 42.7 and 51.7 ppm, respectively. Furthermore, two bands at 1682 cm^{-1} and 1734 cm^{-1} corresponding to the carbonyl groups can be observed in the IR spectrum.

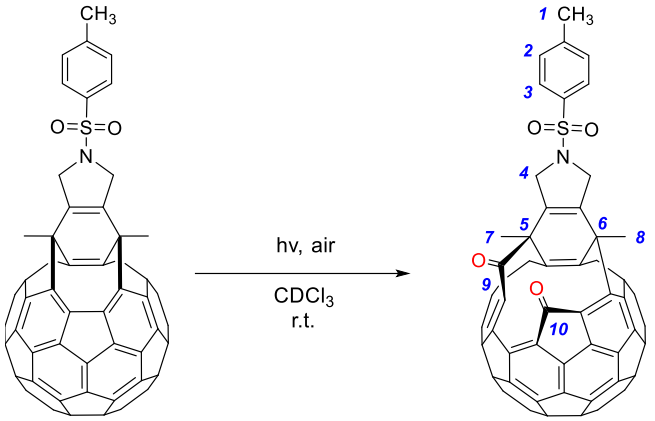

2a **5**

Scheme 3. Oxidative cleavage of bis(fulleroid) derivative **2a**. Arbitrary numbering shown in blue.

Electrochemical behavior of fulleroid derivatives 4b, 4c and 5. The electrochemical behavior of compounds **4b**, **4c** and **5** was studied by cyclic voltammetry to complete their characterization, and to ascertain the effect of the structural modifications introduced in the electron accepting properties of the resulting fulleroadducts with respect to C_{60} (Table 2).

Table 2. Redox potentials of fulleroids **2a, 4b**, **4c**, **5** and C_{60}. [a]

Entry	Compound	E^1_{red}	E^2_{red}	E^3_{red}
1	C_{60}	-1.109	-1.514	-2.009
2	**2a**	-1.213	-1.626	
3	**4b**	-1.228	-1.633	
4	**4c**	-1.211	-1.594	
5	**5**	-0.987	-1.370	

[a] $E_{½}$ in V vs Fc/Fc^+, 0.2 mM C_{60}/**2a**/**4b-c**/**5** and 0.1 M $Bu_4N^+ClO_4^-$ in *o*-dichlorobenzene, SCE reference electrode, Pt working electrode, Pt wire auxiliary electrode, scan rate 50 $mV.s^{-1}$, 25 °C).

All the compounds studied showed two fully reversible reduction waves under the experimental settings employed, corresponding to sequential one electron reduction of the fullerenic core. As expected, the partial disruption of conjugation in bis(fulleroids) **2**, **4b** and **4c** results in a cathodic shift with respect to C_{60}. The obtained potentials compare favorably with structurally analogous bis(fulleroids).[4a] Moreover, the introduction of electro- or photoactive moieties as in **4b/c** does not significantly alter the overall redox properties (compare entries 2-4 in Table 2), indicating that our synthetic scheme is a reliable entry into such fullerene dyads. Conversely, dicarbonyl derivative **5** is more easily reduced than C_{60}, and displays a redox behavior akin to that of previously obtained open-cage fullerenes with homologous π structure.[4a]

Computational study of the reaction mechanism. We completed our study by evaluating computationally the reaction mechanism that transforms **1a** into **2a**, in a process catalyzed by Rh(Tol-BINAP)$^+$ (**P1** = Tol-BINAP in Table 1). The calculated Gibbs reaction profile at the M06-D3/cc-pVTZ-PP//B3LYP-D3/cc-pVDZ-PP level of theory (see Computational Methods for a detailed description) of the determined reaction mechanism is depicted in Figure 3. To reduce the computational effort required, the tosyl group present in the experimental diyne was substituted by a mesyl group. Moreover, the tolyl groups of the catalyst were substituted by methyl groups, since it is generally accepted that PMe_3 is a better model of PPh_3 than PH_3.[17] Finally, the naphthalene moieties were modelled by benzene units (ligand **P9**, see inset of Figure 2). Because it is likely that the reduction considered in our models does not affect critically their chemical behavior, we are confident that the conclusions reached with our model systems should be still valid for the real systems.

The steps of the first part of the reaction (from **A0** to **A5**) correspond to the classic [2+2+2] reaction mechanism. The reaction starts with the coordination of the two triple bonds of diyne of **1a** with Rh(**P9**)$^+$ to form the 16-electron **A1** intermediate and releasing 15.9 kcal/mol. Then, the oxidative coupling takes place through **TS A1A2** with a Gibbs energy barrier of 25.7 kcal/mol, to form rhodacyclopentadiene intermediate **A2** in an exergonic process by 5.1 kcal/mol. The large difference between double C=C (1.345 Å) and single C-C (1.481 Å) bond lengths in intermediate **A2** indicates localization of the π-electron density and lack of aromaticity.[18] For this transformation (**A1** to **A2**), which is the rate determining step in the catalytic cycle, we have explored the influence of using a more realistic model of our catalyst (see Figure S5 in the SI). In particular, we have substituted the methyl groups of our Rh(**P9**)$^+$ model, shown in Figure 3, by phenyl groups. The changes in the Gibbs energy barrier and Gibbs reaction energies for this oxidative coupling process, when going from the Rh(**P9**)$^+$ model to the more realistic model, are less than 2 kcal/mol. This is an indication that our model catalyst is appropriate for the present study.

Coordination of **A2** to a [6,6] bond of C_{60} to yield **A3** is an endergonic process that requires 10.0 kcal/mol. In **A3**, C_{60} is coordinated to Rh occupying an axial position of a distorted trigonal bipyramid. The insertion of C_{60} into the Rh-C(sp^2) bond results in the formation of the rhodabicyclo[3.2.0]heptadiene intermediate **A4** in a step that has a Gibbs barrier of 5.9 kcal/mol and releases 1.8 kcal/mol. The next step corresponds to the formation of intermediate **A5**, which is formed by a reductive elimination process that has to overcome a very low Gibbs energy barrier of 3.2 kcal/mol and is exergonic by 26.8 kcal/mol. In **A5**, Rh is coordinated to both the cyclohexadiene and C_{60} moieties. We also explored the formation of **A5** through rhodacycloheptadiene intermediate **A5'** (Supporting Information, Figure S1) followed by reductive elimination through **TSA5'A5**. This transformation has to surmount a Gibbs energy barrier of 21.2 kcal/mol and it is slightly exergonic by 2.7 kcal/mol, and, consequently, this alternative route through intermediate **A5'** is not competitive and was ruled out. Finally, we also analyzed the possible formation of a rhodanorbonene complex through a rhodium-mediated [4+2] cycloaddition but all our attempts to find

this intermediate failed. It is worth noting that with Wilkinson's catalyst the same reaction mechanism was found, except for the insertion step which leads in this case to a rhodacycloheptadiene intermediate analogous to **A5'** (Schore's mechanism)[19] without formation of a rhodabicyclo[3.2.0]heptadiene intermediate **A4**.[13]

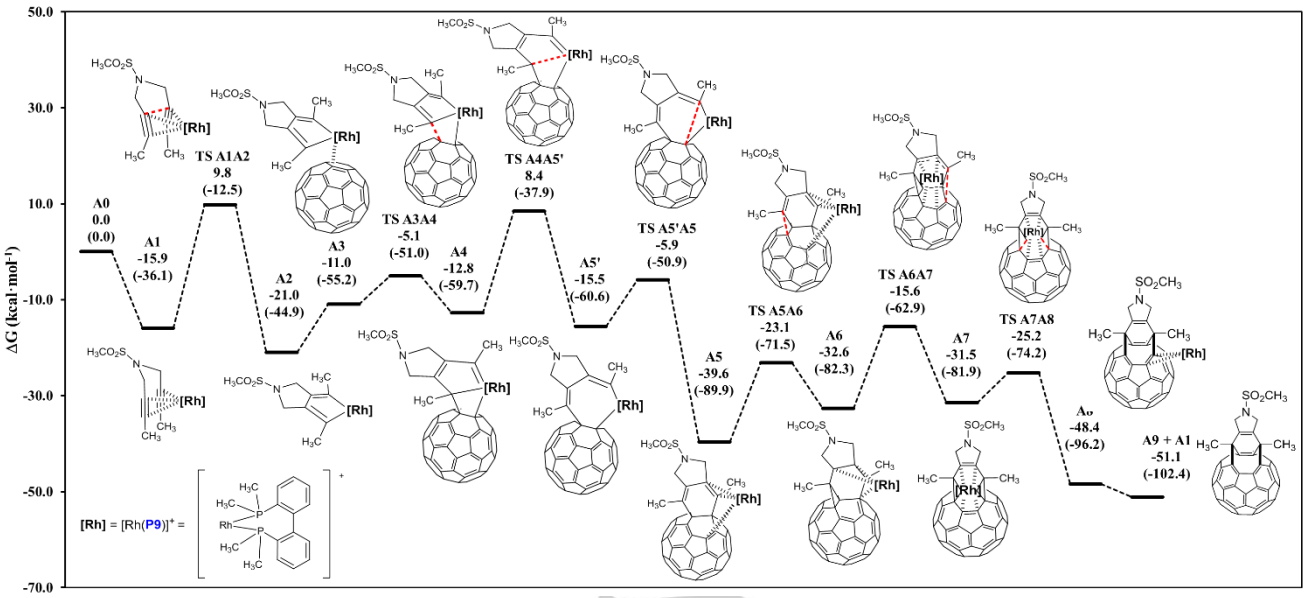

Figure 3. M06-D3/cc-pVTZ-PP//B3LYP-D3/cc-pVDZ-PP Gibbs energy profile of the [2+2+2] cycloaddition reaction of C_{60} and a model of non-terminal tethered diyne **1a** to yield the cyclohexadiene-fused C_{60} derivative **A5** followed by fullerene cage opening to form **A9**. Energies in parenthesis are electronic energies. All relative energies in kcal/mol are given relative to A0 (C_{60} + catalyst + **1a**).

In summary, the [2+2+2] cycloaddition that produces **A5** from **A0** has an energetic span[20] between the turnover frequency (TOF) determining intermediate (TDI, **A1**) and TOF determining transition state (TDTS, **TS A1A2**) of 25.7 kcal/mol. This is in accordance with most [2+2+2] cycloadditions in which the rate determining step (rds) is the oxidative coupling.

We also analyzed another reaction path that transforms **A0** into **A4**. In this alternative pathway (Figure S2, see SI), the oxidative coupling occurs between one alkyne group of **1a** and C_{60} to form a cyclopentene intermediate. Then, the insertion of the second alkyne takes place in a Rh-C(sp^2) bond to form rhodacycloheptadiene **A4**. This alternative pathway has an energetic span between the TDI (**A5**) and TDTS (**TS B1B2**) of 36.5 kcal/mol and, therefore, has been discarded as a possible reaction pathway.

Release of the cyclohexadiene-fused C_{60} from **A5** allows recovery of **A1** to restart the catalytic cycle. The dissociation process releases 8.9 kcal/mol. However, the cyclohexadiene-fused C_{60} adduct is not the final product of the reaction, and it evolves to generate the corresponding bis(fulleroid). We explored different scenarios for the formation of this open-cage fullerene product. First, we considered a [4+4]/retro-[2+2+2] sequence of cycloadditions in the isolated cyclohexadiene-fused C_{60} adduct. The linear transit of the [4+4] cycloaddition in the singlet state shows that this process has a barrier of about 50 kcal/mol (see Figure S3 in the SI). This result is not unexpected since it is well-known that [4+4] cycloadditions are thermally forbidden by the Woodward-Hoffmann rules.[21] In the triplet state, this barrier is reduced to ca. 13 kcal/mol. Therefore, the combination of [4+4] and retro-[2+2+2] cycloadditions would be possible under photoexcitation of the cyclohexadiene derivative. A similar scenario occurs when a stepwise di-π-methane rearrangement is considered,[22] with formation of a singlet biradical **C2** (see Figure S4). For this di-π-methane rearrangement mechanism, we also analyzed the reaction in both the open-shell singlet and triplet excited states. In fact, a bis(fulleroid) species was photochemically synthesized for the first time by Rubin et al. in 1996 from a cyclohexadiene derivative of C_{60}.[6c,23] The singlet excited state of the cyclohexadiene-fused C_{60} adduct is readily populated by photoexcitation. The triplet state can be populated from the singlet excited state followed by intersystem crossing (ISC). It has been reported that the ISC from the first singlet excited state to the first triplet excited state (S_1 to T_1) occurs with high efficiency in C_{60}, mainly due to the small splitting between these two states as well as the large spin-orbital interaction in the spherical cage.[24] As shown in Figure S4, the di-π-methane rearrangement mechanism in both the singlet and triplet excited states is possible with relatively low barriers. In the triplet state, the rds step is the formation of the first biradical intermediate with a closed cyclopropane ring, and has a barrier of 22.3 kcal/mol. Once this intermediate is formed, an ISC brings it to the singlet ground state. From here, the closed-shell singlet [5,6] (bis)methanofullerene species containing two cyclopropane rings is formed with a barrier of only 3.3 kcal/mol. Finally, a thermally allowed retro-[2+2+2] cycloaddition takes place with a barrier of 2.0 kcal/mol to yield the final [5,6] open bis(fulleroid)product. The

greater stability of the bis(fulleroid)product as compared to the (bis)methanofullerene intermediate can be attributed to a) release of ring strain upon opening of the two cyclopropyl rings which are fused to C_{60} pentagons, and b) retention of the 60π electron spherical conjugation and homoaromaticity.[22] The latter relates to the fact that open [5,6] isomers avoid localization of double bonds in pentagonal rings.[25]

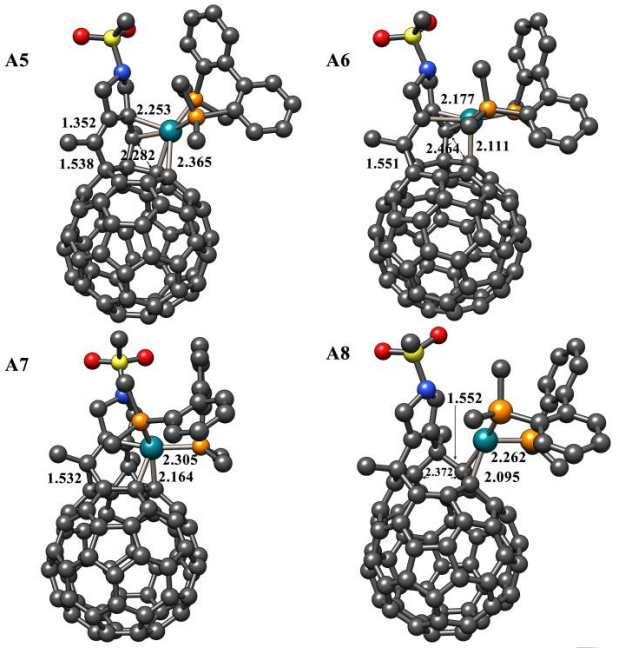

Figure 4. Structure of intermediates **A5**, **A6**, **A7** and **A8**. Hydrogen atoms have been omitted for clarity. Bond distances reported in Å.

Taken together, this data shows that neither the di-π-methane rearrangement pathway nor the [4+4]/retro-[2+2+2] reaction mechanism can explain the formation of the final bis(fulleroid) product without photoexcitation. Furthermore, it is noteworthy that very similar cyclohexadiene derivatives of C_{60} previously reported by Cheng et al. required UV (λ=350 nm) irradiation for 2 h to rearrange into the corresponding bis(fulleroids).[9] Since we have not employed photoexcitation in our system, a reaction path taking place in the ground state must be operative. At this point, it is convenient to remember that the presence of metals in a formal cycloaddition can (i) transform pericyclic reactions into stepwise processes,[26] or (ii) -within a concerted pathway- modify the formal topology of orbital symmetry-allowed mechanisms by means of the participation of the orbitals provided by the metallic center.[27] With these ideas in mind, we investigated the transformation of **A5** to **A9** catalyzed by Rh(**P9**)$^+$. As shown in Figure 3, the reaction mechanism that we found follows a Rh-catalyzed di-π-methane rearrangement pathway. Thus, conversion of the cyclohexadiene-fused C_{60} intermediate **A5** to the [5,6] (bis)methanofullerene intermediate **A7** is a stepwise process in which, first, a cyclopropane ring is formed to yield **A6** (Gibbs barrier of 16.5 kcal/mol, Gibbs reaction energy of 7.0 kcal/mol). In **A6**, Rh is η^4-coordinated to the methanofullerene (Figure 4), thus stabilizing the allyl radical formed. The second cyclopropane ring formation has to surmount a Gibbs energy barrier of 17.0 kcal/mol and is endergonic by 1.1 kcal/mol. Therefore, conversion of **A5** into [5,6] (bis)methanofullerene intermediate **A7** has an overall Gibbs energy barrier of 24.0 kcal/mol (**TS A6A7** with respect to **A5**) and is endergonic by 8.1 kcal/mol. **A7** is a [5,6] (bis)methanofullerene that is η^4-coordinated to Rh by one [5,6] bond of the fullerene cage and by the double bond of the cyclochexene addend. Opening of the two fullerene C–C bonds of the cyclopropane moieties to form the bis(fulleroid)product **A8** coordinated to Rh(**P9**)$^+$ takes place concertedly in a process that requires to surpass a barrier of 6.3 kcal/mol and releases 16.9 kcal/mol. Intermediate **A8** is η^2-coordinated to one of the double bonds at the rim of the 8-membered hole of the fullerene. This structure is analogous to the X-ray structure reported by Rubin et al. for a similar complex. In the latter case, a Co(Cp) fragment is η^4-coordinated to the (bis)fulleroid.[6c] Final liberation of product **A9** and recovery of **A1** is slightly exergonic by -2.8 kcal/mol. Overall, once a Rh(**P9**)$^+$-catalyzed di-π-methane rearrangement pathway is considered, the barriers become relatively low and the full process is exergonic. Therefore, we demonstrated that the evolution from cyclohexadiene-fused C_{60} intermediate to the bis(fulleroid) product is possible without irradiation as far as the catalyst is present in the reaction. This conversion occurs through a di-π-methane rearrangement pathway followed by a retro-[2+2+2] cycloaddition. This last step is thermally allowed and can be performed either in the presence or in the absence of catalyst (see Figure S4).

Conclusions

In conclusion, we have developed an efficient cascade process leading to functionalized open-cage fullerene derivatives. The method is modular and catalytic in rhodium, providing the corresponding fulleroadducts in good to moderate yields starting from simple diyne precursors. The resulting fulleroadducts can be decorated with varied functionality, including haloarene handles for further functionalization through Pd-catalyzed cross-coupling reactions. Overall, this reaction sequence provides a versatile entry to donor-acceptor fulleroid dyads based on catalytic methods. DFT calculations show that the reaction takes place via a Rh-catalyzed [2+2+2] cycloaddition through a rhodabicyclo[3.2.0]heptadiene intermediate to yield a cyclohexadiene-fused C_{60} intermediate. This intermediate evolves to the final bis(fulleroid) product following a Rh-catalyzed di-π-methane rearrangement pathway followed by a retro-[2+2+2] cycloaddition. The initial oxidative coupling step of the Rh-catalyzed [2+2+2] cycloaddition is the rate-determining step of the whole reaction pathway.

Experimental Section

Representative procedure for the preparation of 2a. In a 10 mL capped vial, a mixture of $[Rh(cod)_2]BF_4$ (2.8 mg, 0.007 mmol, 0.1 equiv.) and Tol-BINAP (4.8 mg, 0.007 mmol, 0.1 equiv.) was purged with nitrogen and dissolved in anhydrous CH_2Cl_2 (4 mL). Hydrogen gas was bubbled into the catalyst solution and the mixture was stirred for 30 min. The resulting mixture was concentrated to dryness. Anhydrous *o*-dichlorobenzene (10 mL) was added and the resulting solution was then transferred via syringe into a solution of C_{60} (50 mg, 0.07 mmol, 1 equiv.) and

diyne **1a** (96 mg, 0.35 mmol, 5 equiv.) in anhydrous *o*-dichlorobenzene (40 mL, final [C_{60}] = 1.4 mM) preheated to 90 ºC. The resulting mixture was heated to 90 ºC and stirred for 4h. The solvent was removed under reduced pressure and the crude reaction mixture was purified by column chromatography on silica gel using toluene as the eluent, affording unreacted C_{60} (25 mg) and **2a** (36 mg, 52% yield, 98% yield based on consumed C_{60}) as a dark brown solid. Analytical samples were prepared by washing **2a** with *n*-pentane (3 x 2 mL).

Computational Methods

Geometries of all stationary points were optimized without symmetry constraint with the Gaussian 09 program[28] using the DFT B3LYP hybrid exchange-correlation functional.[29] The all-electron cc-pVDZ basis set[30] was employed for non-metal atoms and the cc-pVDZ-PP basis set[31] containing an effective core relativistic pseudopotential was used for Rh. The electronic energy was improved by performing single point energy calculations with the cc-pVTZ (cc-pVTZ-PP for Rh) basis set and the M06 functional[32] and including solvent effects corrections of a *o*-dichlorobenzene solution computed with the solvent model based on density (SMD) continuum solvation model.[33] The D3 Grimme energy corrections for dispersion[34] with the original damping function were added in all B3LYP/cc-pVDZ-PP and M06/cc-pVTZ-PP calculations. Analytical Hessians were computed to determine the nature of stationary points (one and zero imaginary frequencies for TSs and minima, respectively) and to calculate unscaled zero-point energies (ZPEs) as well as thermal corrections and entropy effects using the standard statistical-mechanics relationships for an ideal gas.[35] These two latter terms were computed at 363.15 K and 1 atm to provide the reported relative Gibbs energies. As a summary, the reported Gibbs energies contain electronic energies including solvent effects calculated at the M06-D3/cc-pVTZ-PP//B3LYP-D3/cc-pVDZ-PP level together with gas phase thermal and entropic contributions computed at 363.15 K and 1 atm with the B3LYP-D3/cc-pVDZ-PP method. To reduce the computational cost of the calculations, the tosyl group present in model compound **2a** was substituted by a mesyl group, the four tolyl groups present in the Rh(I)-Tol-BINAP catalyst were substituted by methyl groups, and the binaphthyl core was substituted by biphenyl (ligand **P9**, see Figure 2).

Acknowledgements

We are grateful for the financial support by the Spanish Ministry of Economy and Competitivity (MINECO, Projects CTQ2017-85341-P and CTQ2017-83587-P, FPI predoctoral grant to A.A., RyC contract RYC2012-11112 to A.L.) and the Generalitat de Catalunya (Project 2017-SGR-39, Xarxa de Referència en Química Teòrica i Computacional, ICREA Academia 2014 prize for M.S.). The EU under the FEDER grant UNGI10-4E-801 has also funded this research.

Conflict of interest

The authors declare no conflict of interest.

Keywords: Open-cage fullerenes • Cycloaddition reactions • Rhodium • Catalysis • DFT calculations •

[1] For monographies, see: a) F. Langa, J. F. Nierengarten, *Fullerenes: Principles and Applications: Edition 2*, The Royal Society of Chemistry, Cambridge, **2012**; b) F. Cataldo, T. da Ros, *Medicinal chemistry and pharmacological potential of fullerenes and carbon nanotubes*. 1ed. Springer, **2008**; c) A. Hirsch, M. Brettreich, *Fullerenes: Chemistry and Reactions,* Wiley-VCH, Weinheim, **2005**. For selected reviews see: d) S.-E. Zhu, F. Li, G.-W. Wang, *Chem. Soc. Rev.* **2013**, *42*, 7535-7570; e) M. D. Tzirakis, M. Orfanopoulos, *Chem. Rev.* **2013**, *113*, 5262-5321; f) K. Itami, *Chem. Rec.* **2011**, *11*, 226-235; g) F. Giacalone, N. Martín, *Adv. Mater.* **2010**, *22*, 4220-4248; h) Y. Matsuo, E. Nakamura, *Chem. Rev.* **2008**, *108*, 3016-3028; i) C. Thilgen, F. Diederich, *Chem. Rev.* **2006**, *106*, 5049-5135; j) F. Giacalone, N. Martín, *Chem. Rev.* **2006**, *106*, 5136-5190; k) M. Bendikov, F. Wudl, D. F. Perepichka, *Chem. Rev.* **2004**, *104*, 4891-4946; l) E. Nakamura, H. Isobe, *Acc. Chem. Res.* **2003**, *36*, 807-815; m) L. Echegoyen, L. E. Echegoyen, *Acc. Chem. Res.* **1998**, *31*, 593-601; n) M. Prato, *J. Mater. Chem.* **1997**, *7*, 1097-1109.

[2] For selected reviews see: a) E. Castro, J. Murillo, O. Fernandez-Delgado, L. Echegoyen, *J. Mater. Chem. C,* **2018**, *6*, 2635-2651; b) R. Ganesamoorthy, G. Sathiyan, P. Sakthivel, *Solar Energy Mater. Sol. Cells* **2017**, *161*, 102-148; c) M. Rudolf, S. V. Kirner, D. M. Guldi, *Chem. Soc. Rev.* **2016**, *45*, 612-630; d) M. Rudolf, S. Wolfrum, D. M. Guldi, L. Feng, T. Tsuchiya, T. Akasaka, L. Echegoyen, *Chem. Eur. J.* **2012**, *18*, 5136-5148; e) Y. Matsuo, *Chem. Lett.* **2012**, *41*, 754-759; f) Y. Li, *Acc. Chem. Res.* **2012**, *45*, 723-733; g) C.-Z. Li, H.-L. Yip, A. K. Y. Jen, *J. Mater. Chem.* **2012**, *22*, 4161-4177; h) Y. He, Y. Li, *Phys. Chem. Chem. Phys.* **2011**, *13*, 1970-1983; i) J. L. Delgado, N. Martin, P. de la Cruz, F. Langa, *Chem. Soc. Rev.* **2011**, *40*, 5232-5241; j) J. L. Delgado, P.-A. Bouit, S. Filippone, M. A. Herranz, N. Martin, *Chem. Commun.* **2010**, *46*, 4853-4865; k) J. Roncali, *Acc. Chem. Res.* **2009**, *42*, 1719-1730; l) D. M. Guldi, B. M. Illescas, C. M. Atienza, M. Wielopolski, N. Martin, *Chem.l Soc. Rev.* **2009**, *38*, 1587-1597; m) J. Chen, Y. Cao, *Acc. Chem. Res.* **2009**, *42*, 1709-1718; n) B. M. Illescas, N. Martín, *C. R. Chimie* **2006**, *9*, 1038-1050.

[3] a) S. Vidal, M. Izquierdo, S. Alom, M. Garcia-Borras, S. Filippone, S. Osuna, M. Sola, R. J. Whitby, N. Martin, *Chem. Commun.* **2017**, *53*, 10993-10996; b) Y. Hashikawa, M. Murata, A. Wakamiya, Y. Murata, *J. Am. Chem. Soc.* **2016**, *138*, 4096-4104; c) E. E. Maroto, J. Mateos, M. Garcia-Borràs, S. Osuna, S. Filippone, M. Á. Herranz, Y. Murata, M. Solà, N. Martín, *J. Am. Chem. Soc.* **2015**, *137*, 1190-1197; d) L. Shi, L. Gan, *J. Phys. Org. Chem.* **2013**, *26*, 766-772; e) G. C. Vougioukalakis, M. M. Roubelakis, M. Orfanopoulos, *Chem. Soc. Rev.* **2010**, *39*, 817-844; f) N. J. Turro, J. Y. C. Chen, E. Sartori, M. Ruzzi, A. Marti, R. Lawler, S. Jockusch, J. López-Gejo, K. Komatsu, Y. Murata, *Acc. Chem. Res.* **2010**, *43*, 335-345; g) L. Gan, D. Yang, Q. Zhang, H. Huang, *Adv. Mater.* **2010**, *22*, 1498-1507; h) M. Murata, Y. Murata, K. Komatsu, *Chem. Commun.* **2008**, 6083-6094.;

[4] a) M. Murata, Y. Morinaka, Y. Murata, O. Yoshikawa, T. Sagawa, S. Yoshikawa, *Chem. Commun.* **2011**, *47*, 7335-7337; b) C.-P. Chen, Y.-W. Lin, J.-C. Horng, S.-C. Chuang, *Adv. Energy Mater.* **2011**, *1*, 776-780; c) S. H. Park, C. Yang, S. Cowan, J. K. Lee, F. Wudl, K. Lee, A. J. Heeger, *J. Mater. Chem.* **2009**, *19*, 5624-5628.

[5] a) Z. Zhou, N. Xin, L. Gan, *Chem. Eur. J.* **2018**, *24*, 451-457; b) Y. Li, L. Gan, *Chem. Eur. J.* **2017**, *23*, 10485-10490.

[6] Selected references: a) S.-i. Iwamatsu, P. S. Vijayalakshmi, M. Hamajima, C. H. Suresh, N. Koga, T. Suzuki, S. Murata, *Org. Lett.* **2002**, *4*, 1217-1220; b) Y. Murata, N. Kato, K. Komatsu, *J. Org. Chem.* **2001**, *66*, 7235-7239; c) M.-J. Arce, A. L. Viado, Y.-Z. An, S. I. Khan, Y. Rubin, *J. Am. Chem. Soc.* **1996**, *118*, 3775-3776.

[7] For reviews involving alkenes and allenes in transition-metal-catalysed [2+2+2] cycloaddition reactions, see: a) A. Lledo, A. Pla-Quintana, A. Roglans, *Chem. Soc. Rev.* **2016**, *45*, 2010-2023; b) G. Domínguez, J.

Pérez-Castells, *Chem. Eur. J.* **2016**, *22*, 6720-6739; For a monography covering the whole of [2+2+2] cycloaddition chemistry, see: (c) K. Tanaka, *Transition-Metal-Mediated Aromatic Ring Construction*, 1ed. John Wiley & Sons, Inc. **2013**.

[8] a) I. Fernández, M. Solà, F. M. Bickelhaupt, *Chem. Eur. J.* **2013**, *19*, 7416-7422; b) W. Śliwa, *Fullerene Science and Technology* **1995**, *3*, 243-281; c) M. Solá, J. Mestres, J. Martí, M. Duran, *Chem. Phys. Lett.* **1994**, *231*, 325-330.

[9] T.-Y. Hsiao, K. C. Santhosh, K.-F. Liou, C.-H. Cheng, *J. Am. Chem. Soc.* **1998**, *120*, 12232-12236.

[10] H. Inoue, H. Yamaguchi, T. Suzuki, T. Akasaka, S. Murata, *Synlett* **2000**, *2000*, 1178-1180;

[11] K.-F. Liou, C.-H. Cheng, *J. Chem. Soc., Chem. Commun.* **1995**, 1603-1604.

[12] a) E. Haraburda, M. Fernández, A. Gifreu, J. Garcia, T. Parella, A. Pla-Quintana, A. Roglans, *Adv. Synth. Catal.* **2017**, *359*, 506-512; b) D. Cassú, T. Parella, M. Solà, A. Pla-Quintana, A. Roglans, *Chem. Eur. J.* **2017**, *23*, 14889-14899; c) M. Fernández, M. Parera, T. Parella, A. Lledó, J. Le Bras, J. Muzart, A. Pla-Quintana, A. Roglans, *Adv. Synth. Catal.* **2016**, *358*, 1848-1853; d) E. Haraburda, A. Lledó, A. Roglans, A. Pla-Quintana, *Org. Lett.* **2015**, *17*, 2882-2885; e) E. Haraburda, Ò. Torres, T. Parella, M. Solà, A. Pla-Quintana, *Chem. Eur. J.* **2014**, *20*, 5034-5045; f) T. León, M. Parera, A. Roglans, A. Riera, X. Verdaguer, *Angew. Chem. Int. Ed.* **2012**, *51*, 6951-6955; g) A. Dachs, A. Roglans, M. Solà, *Organometallics* **2011**, *30*, 3151-3159; h) A. Dachs, A. Pla-Quintana, T. Parella, M. Solà, A. Roglans, *Chem. Eur. J.* **2011**, *17*, 14493-14507; i) S. Brun, L. Garcia, I. Gonzalez, A. Torrent, A. Dachs, A. Pla-Quintana, T. Parella, A. Roglans, *Chem. Commun.* **2008**, 4339-4341; j) A. Torrent, I. González, A. Pla-Quintana, A. Roglans, M. Moreno-Mañas, T. Parella, J. Benet-Buchholz, *J. Org. Chem.* **2005**, *70*, 2033-2041.

[13] A. Artigas, A. Lledó, A. Pla-Quintana, A. Roglans, M. Solà, *Chem. Eur. J.* **2017**, *23*, 15067-15072.

[14] Selected references: a) Z.-Y. Wu, R. Zhong, F.-Z. Yang, *J. Organomet. Chem.* **2017**, *840*, 75-81; b) C.-H. Andersson, L. Nyholm, H. Grennberg, *Dalton Trans.* **2012**, *41*, 2374-2381; c) M. Á. Herranz, B. Illescas, N. Martín, C. Luo, D. M. Guldi, *J. Org. Chem.* **2000**, *65*, 5728-5738; d) D. M. Guldi, M. Maggini, G. Scorrano, M. Prato, *J. Am. Chem. Soc.* **1997**, *119*, 974-980.

[15] Selected references: a) G. Zaragoza-Galán, J. Ortíz-Palacios, B. Valderrama, A. Camacho-Dávila, D. Chávez-Flores, V. Ramos-Sánchez, E. Rivera, *Molecules* **2014**, *19*, 352; b) Y. Matsuo, K. Morita, E. Nakamura, *Chem. As. J.* **2008**, *3*, 1350-1357; c) F. Hauke, A. Hirsch, S. Atalick, D. Guldi, *Eur. J. Org. Chem.* **2005**, *2005*, 1741-1751.

[16] a) Y. Murata, M. Murata, K. Komatsu, *Chem. Eur. J.* **2003**, *9*, 1600-1609; b) M. Yasujiro, K. Koichi, *Chem. Lett.* **2001**, *30*, 896-897; c) Y. Murata, M. Murata, K. Komatsu, *J. Org. Chem.* **2001**, *66*, 8187-8191; d) H. Inoue, H. Yamaguchi, S.-i. Iwamatsu, T. Uozaki, T. Suzuki, T. Akasaka, S. Nagase, S. Murata, *Tetrahedron Lett.* **2001**, *42*, 895-897.

[17] a) T. Kegl, *RSC Advances* **2015**, *5*, 4304-4327; b) H. Xie, Q. Sun, G. Ren, Z. Cao, *J. Org. Chem.* **2014**, *79*, 11911-11921; c) C. Flener Lovitt, G. Frenking, G. S. Girolami, *Organometallics* **2012**, *31*, 4122-4132.

[18] a) A. A. Dahy, N. Koga, *Organometallics* **2015**, *34*, 4965-4974; b) J. H. Hardesty, J. B. Koerner, T. A. Albright, G.-Y. Lee, *J. Am. Chem. Soc.* **1999**, *121*, 6055-6067.

[19] N. E. Schore, *Chem. Rev.* **1988**, *88*, 1081-1119.

[20] a) S. Kozuch, S. Shaik, *Acc. Chem. Res.* **2011**, *44*, 101-110; b) S. Kozuch, S. Shaik, *J. Phys. Chem. A* **2008**, *112*, 6032-6041.

[21] (a) R. B. Woodward, R. Hoffmann, *The Conservation of Orbital Symmetry*, Academic Press: New York, **1970**; b) R. Hoffmann, R. B. Woodward, *Acc. Chem. Res.* **1968**, *1*, 17-22; c) R. B. Woodward, R. Hoffmann, *J. Am. Chem. Soc.* **1965**, *87*, 395-397.

[22] C. H. Suresh, P. S. Vijayalakshmi, S.-i. Iwamatsu, S. Murata, N. Koga, *J. Org. Chem.* **2003**, *68*, 3522-3531.

[23] Y. Rubin, *Chem. Eur. J.* **1997**, *3*, 1009-1016.

[24] R. R. Hung, J. J. Grabowski, *J. Phys. Chem.* **1991**, *95*, 6073-6075.

[25] M. Cases, M. Duran, J. Mestres, N. Martín, M. Solà, *Fullerenes for the New Millennium*, (P. V. Kamat, D. M. Guldi, K. M. Kadish, Eds.), The Electrochemical Society, Inc., Pennigton, vol. 11, **2001**.

[26] J. M. Hoyt, V. A. Schmidt, A. M. Tondreau, P. J. Chirik, *Science* **2015**, *349*, 960-963.

[27] M. Mauksch, S. B. Tsogoeva, *Chem. Eur. J.* **2016**, *22*, 13916-13926.

[28] Gaussian 09, Revision E.01, M. J. Frisch, G. W. Trucks, H. B. Schlegel, G. E. Scuseria, M. A. Robb, J. R. Cheeseman, G. Scalmani, V. Barone, G. A. Petersson, H. Nakatsuji, X. Li, M. Caricato, A. V. Marenich, J. Bloino, B. G. Janesko, R. Gomperts, B. Mennucci, H. P. Hratchian, J. V. Ortiz, A. F. Izmaylov, J. L. Sonnenberg, Williams, F. Ding, F. Lipparini, F. Egidi, J. Goings, B. Peng, A. Petrone, T. Henderson, D. Ranasinghe, V. G. Zakrzewski, J. Gao, N. Rega, G. Zheng, W. Liang, M. Hada, M. Ehara, K. Toyota, R. Fukuda, J. Hasegawa, M. Ishida, T. Nakajima, Y. Honda, O. Kitao, H. Nakai, T. Vreven, K. Throssell, J. A. Montgomery Jr., J. E. Peralta, F. Ogliaro, M. J. Bearpark, J. J. Heyd, E. N. Brothers, K. N. Kudin, V. N. Staroverov, T. A. Keith, R. Kobayashi, J. Normand, K. Raghavachari, A. P. Rendell, J. C. Burant, S. S. Iyengar, J. Tomasi, M. Cossi, J. M. Millam, M. Klene, C. Adamo, R. Cammi, J. W. Ochterski, R. L. Martin, K. Morokuma, O. Farkas, J. B. Foresman and D. J. Fox, Gaussian, Inc., Wallingford CT, **2009**.

[29] a) P. J. Stephens, F. J. Devlin, C. F. Chabalowski, M. J. Frisch, *J. Phys. Chem.* **1994**, *98*, 11623-11627; b) A. D. Becke, *J. Chem. Phys.* **1993**, *98*, 5648-5652; c) C. Lee, W. Yang, R. G. Parr, *Phys. Rev.* **1988**, *37*, 785-789.

[30] a) D. E. Woon, T. H. Dunning Jr., *J. Chem. Phys.* **1993**, *98*, 1358-1371; b) T. H. Dunning Jr., *J. Chem. Phys.* **1989**, *90*, 1007-1023.

[31] K. A. Peterson, D. Figgen, M. Dolg, H. Stoll, *J. Chem. Phys.* **2007**, *126*, 124101.

[32] Y. Zhao, D. G. Truhlar, *J. Chem. Phys.* **2006**, *125*, 194101.

[33] A. V. Marenich, C. J. Cramer, D. G. Truhlar, *J. Phys. Chem. B* **2009**, *113*, 6378-6396.

[34] S. Grimme, J. Antony, S. Ehrlich, H. Krieg, *J. Chem. Phys.* **2010**, *132*, 154104.

[35] P. Atkins, J. De Paula, in *Phys. Chem.*, Oxford University Press, Oxford, **2006**.

Entry for the Table of Contents

Layout 2:

FULL PAPER

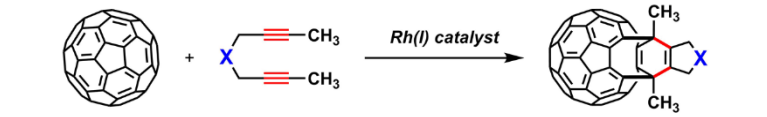

■ Catalytic conditions ■ Direct access to bis(fulleroids) ■ Yields up to 60%
■ Further functionalization ■ Mechanism elucidation ■ Rh(I)-catalyzed ring opening

A novel methodology to transform C_{60} into a variety of open-cage fullerene derivatives employing rhodium(I) catalysis has been developed. DFT calculations show this transformation takes place though a partially intermolecular [2+2+2] cycloaddition reaction between diynes and C_{60} followed by Rh(I)-catalyzed cage-opening.

Albert Artigas, Anna Pla-Quintana, Agustí Lledó, Anna Roglans,* and Miquel Solà*[]*

Page No. – Page No.

Expeditious Preparation of Open-Cage Fullerenes by Rhodium(I)-Catalyzed [2+2+2] Cycloaddition of Diynes and C_{60}: an Experimental and Theoretical Study